Mechanism of the Reaction $C_2H_5 + O_2$ from 298 To 680 K

E. W. Kaiser

Ford Motor Company, P.O. Box 2053, Research Laboratory, Mail Drop 3083/SRL, Dearborn, Michigan 48121-2053

Received: August 8, 2001; In Final Form: November 2, 2001

The reaction $C_2H_5 + O_2$ has been studied by steady-state photolysis of mixtures containing Cl_2, C_2H_6, and O_2 over the temperature range 298−680 K at a constant density of 6.8×10^{18} molecules cm^{-3}. Limited experiments were also performed as a function of pressure (200−1300 Torr) at four temperatures. After UV irradiation, the mixtures were analyzed by GC/MS to determine the product yields. The yield of C_2H_4 increases slowly between 298 and 450 K ($E_a \sim 1$ kcal mol^{-1}) and then increases sharply ($E_a \sim 25$ kcal mol^{-1}) reaching a yield of 100(±10)% of the O_2 reaction channel by 630 K. For $T < 450$ K, the C_2H_4 yield depends on the inverse of the pressure, indicating that the ethylene is formed via a chemically activated ($C_2H_5O_2$*) radical as has been observed previously. Above 500 K, the C_2H_4 yield is independent of pressure indicating that a new channel has opened. This is confirmed by the observation that the ratio β (= C_2H_4/C_2H_5Cl) increases sharply (from 0.8 to 3.5) between 450 and 500 K. If the C_2H_5 radical remained the sole source of C_2H_4 (via $C_2H_5O_2$*) throughout the entire temperature range, no sharp break in β would occur. The very small yield of ethylene oxide (2.5% at 660 K) and the excellent carbon balance between C_2H_6 consumed and products formed above 530 K support the formation of C_2H_4 at elevated temperature via both the thermally activated, concerted path ($C_2H_5O_2 \rightarrow C_2H_4 + HO_2$) proposed recently and the chemically activated ($C_2H_5O_2$*) path. The former reaction occurs from a stabilized ethylperoxy radical without passing through a stable hydroperoxyethyl radical. Phenomenological rate constants at the experimental density are presented for the chemically and thermally activated paths to C_2H_4 formation. The data also indicate that the formation of C_2H_4 by direct H-atom abstraction is negligible under the conditions of these experiments [k_{abs}(700 K) $< 1 \times 10^{-13}$ cm^3 $molecule^{-1}$ s^{-1}].

Introduction

The reaction of C_2H_5 with O_2 is of central importance in combustion chemistry because many larger hydrocarbon radicals decompose through β-scission to smaller radicals ending ultimately in ethyl and methyl. Also, ethyl is the smallest radical that shows many of the features of the oxidation of larger alkyl radicals, including the formation of an alkene. The reaction has attracted much interest, both experimental and theoretical. A recent publication[1] of high level ab initio characterizations includes an exhaustive discussion of the history of the studies of this reaction with an extensive list of citations. Two other theoretical analyses applying electronic structure theory, VTST or QRRK, and master equation solutions have also been presented recently.[2,3] At ambient temperature and pressure, addition to form a stabilized ethylperoxy radical via reaction 1 (exothermicity of ∼34 kcal mol^{-1}) is dominant,

$$C_2H_5 + O_2 \leftrightarrow C_2H_5O_2 \qquad (1)$$

At elevated temperature, formation of ethylene is the major product channel. The current experiments investigate the mechanism of the formation of ethylene from reaction 1 over a wide temperature range. In addition, estimates of selected phenomenological rate constants under the conditions studied (constants including an upper limit to the direct H-atom abstraction reaction) will be discussed in the Appendix.

Previous experiments have provided several key observations about reaction 1 and the generation of ethylene: (1) the overall reaction has a negative temperature coefficient up to 1000 K, which spans the regions in which either ethylperoxy radicals or ethylene are the dominant products;[4] (2) ethylene is generated at ambient temperature with an inverse dependence on total pressure up to 10 atm;[5] and (3) as the temperature increases above ambient, the yields of ethylene[6] and HO_2[7] at constant total density first rise slowly (apparent $E_a \sim 1$ kcal) and then rise sharply (apparent $E_a \sim 25$ kcal) between 450 and 600 K. The strong inverse pressure dependence at ambient temperature for pressures above which the overall reaction approaches its high-pressure limit (50 Torr[8]) requires that the ethylene be formed via a chemically activated ethylperoxy radical ($C_2H_5O_2$*), which can be stabilized to ground-state ethylperoxy by collision with the bath gas (named the "prompt" channel in ref 7):

$$C_2H_5 + O_2 \rightarrow C_2H_5O_2^* \rightarrow C_2H_4 + HO_2 \qquad (1a)$$

$$C_2H_5O_2^* + M \rightarrow C_2H_5O_2 + M \qquad (1b)$$

The sharp rise in ethylene yield for temperatures in the range 450−550 K indicates that a new channel has opened. This could be associated with the increasing reversibility of reaction 1 as the temperature increases. Dissociation of ethylperoxy back to reactants leads to the possibility that the increasing ethylene yield may result from multiple passes through the chemically (vibrationally) activated ethylperoxy radical with a small chance of forming ethylene at each pass, thereby increasing the observed ethylene and HO_2 yields, as suggested previously.[6] Two other paths are possible. The first is a thermally activated, concerted

10.1021/jp013089j CCC: $22.00
Published on Web 01/22/2002

elimination of ethylene from the stabilized ethylperoxy radical described by Rienstra-Kiracofe et al.[1] and also discussed in refs 2 and 3,

$$C_2H_5O_2 \rightarrow C_2H_4 + HO_2 \qquad (1c)$$

This does pass through the same transition state as reaction 1a and is not truly a new reaction channel. However, in the remainder of the paper, reaction 1c is considered separately since it requires thermal activation after prior $C_2H_5O_2$ stabilization to proceed to C_2H_4 rather than chemical activation without stabilization as in reaction 1a. The final possibility that has been proposed is a two-step reaction in which ethylperoxy rearranges to hydroperoxyethyl, which decomposes to $C_2H_4 + HO_2$,[9]

$$C_2H_5O_2 \rightarrow C_2H_4O_2H \qquad (1d')$$

$$C_2H_4O_2H \rightarrow C_2H_4 + HO_2 \qquad (1d)$$

All three possibilities produce ethylene as a product. However, reaction 1d proceeds via a stable hydroperoxyethyl radical which could participate in the reaction process by adding another O_2 to the radical site. Thus, this path in particular differs mechanistically from the other two. In this paper, data are presented which shed additional light on the mechanism of C_2H_4 formation from addition of O_2 to C_2H_5 using a relative rate method with final product analysis.

Experiment

In the current studies, two primary reactors were used, both Pyrex cylinders: one 80 cm^3 in volume (2.5 cm i.d. × 17 cm long), and one 40 cm^3 (2.5 cm i.d. × 8 cm). Each reactor was coated with boric acid and exposed repeatedly to stoichiometric, 70 Torr, H_2/O_2 mixtures at 785 K to passivate the surface. Both were equipped with a thermocouple well running the length of the reactor for temperature determination. The shorter reactor had a temperature nonuniformity of approximately 3 K (at 575 K) over its entire length; measurements at other temperatures also show the same nonuniformity as a percentage of the difference between T and ambient temperature [i.e., for this reactor $\Delta T = 0.011(T - 298)$]. The longer reactor had a larger temperature nonuniformity (e.g., 575 ± 10 K) in the region irradiated. For the kinetics experiments, a reactor was placed into a tube oven and the top of the oven was propped open on one side to a height of ~0.8 cm to provide access for photolytic irradiation. A 10 cm length was irradiated, representing the entire 40 cm^3 reactor but only 60% of the 80 cm^3 reactor. Limited experiments were also carried out with a second (uncoated) 40 cm^3 reactor to test for the presence of heterogeneous reactions.

Reactant mixtures containing C_2H_6 (99.99+%), Cl_2 (degassed−99.99% liquid phase), O_2 (99.998%), and N_2 (99.999%) were irradiated for a chosen time by a Sylvania F6T5 BLB fluorescent lamp. The entire contents of the reactor were then removed into a Pyrex transfer flask for capillary gas chromatographic (GC) analysis using a GC/MS instrument (Hewlett-Packard model 6890/5973). The organic species with the exception of CH_2O were measured using a 30 m (0.32 mm) DB-1 capillary column (J&W Scientific) at 35° C and a flame ionization detector (FID). CO_2 and CH_2O were also quantified using this column but with MS detection. CO was separated on a 30 m (0.32 mm) Gas Pro capillary column (J&W Scientific) at −70° C also using the MS detector. Calibration of CH_2O was achieved by thermally decomposing paraformaldehyde to yield CH_2O at a measured pressure in a Pyrex flask. This was then diluted to the desired mole fraction for use in calibration of the GC/MS. This typical standard (~30 ppm) was stable for several days. All other species were also calibrated using pure samples diluted to the desired mole fraction. The linearity of the detectors with changes in species mole fraction was tested and found to be satisfactory for the accuracy of these experiments.

The UV radiation from the lamp dissociates Cl_2 to form Cl atoms which react with C_2H_6 yielding C_2H_5 radicals. The ethyl radicals react with O_2 to form either $C_2H_5O_2$ or C_2H_4 and also with Cl_2 to form C_2H_5Cl. The overall yield of each product is obtained from the final product concentration divided by the amount of C_2H_6 consumed. In these experiments, the yields of C_2H_4, C_2H_5Cl, CH_3CHO, CH_2O, C_2H_4O (ethylene oxide), CO, and CO_2 were determined for ethane consumption between 10 and 50%. C_2H_5OH was observed at lower temperatures but not quantified because of difficulties encountered with nonreproducible loss of ethanol during the sampling and analysis procedures.

Most experiments were carried out with a base mixture of composition: $C_2H_6 = 1.4 \times 10^{16}$ molecules cm^{-3}; $Cl_2 = 2.9 \times 10^{16}$; $O_2 = 6.7 \times 10^{18}$; $N_2 = 0$. Measurements were also taken: (1) with N_2 added to give a total density of 2.7×10^{19}, (2) with Cl_2 increased to 8.7×10^{16}, or (3), with C_2H_6 reduced to 0.5×10^{16}. These experiments assessed the effects of changing the pressure, the Cl_2/O_2 ratio, or the initial C_2H_6 while keeping the other constituent densities the same as in the base mixture. Reducing the initial C_2H_6 density produced no change in the product yields at 567 K, the only temperature for which reduced initial C_2H_6 was tested. Experiments were conducted over the temperature range 298−680 K.

Results

Product Yields. Initially, four experiments were performed on the base mixture at ambient temperature in the passivated 80 cm^3 reactor to compare the yield of the largest product, CH_3CHO, to those measured previously in two detailed product yield experiments using Cl_2 photolysis in the presence of C_2H_6 and air.[10,11] These FTIR experiments showed that CH_3CHO (55−60%), $C_2H_5O_2H$ (25−30%), and C_2H_5OH (15%) were the only significant products observed at low percentages of consumption of ethane:

$$C_2H_5O_2 + C_2H_5O_2 \rightarrow C_2H_5O + C_2H_5O + O_2 \qquad (2)$$

$$C_2H_5O_2 + C_2H_5O_2 \rightarrow C_2H_5OH + CH_3CHO + O_2 \qquad (3)$$

$$C_2H_5O_2 + HO_2 \rightarrow C_2H_5O_2H \text{ (or } C_2H_5O + OH \text{ at elevated temperature)} + O_2 \qquad (4)$$

$$C_2H_5O + O_2 \rightarrow CH_3CHO + HO_2 \qquad (5)$$

Figure 1 presents the yields of CH_3CHO measured in the current ambient temperature measurements and also the yields of the minor products, C_2H_4 (formed from reaction 1a) and C_2H_5Cl:

$$CH_3 + Cl_2 \rightarrow CH_3Cl + Cl \qquad (6)$$

$$C_2H_5 + Cl_2 \rightarrow C_2H_5Cl + Cl \qquad (7)$$

CH_3CHO yields are raw data uncorrected for secondary consumption by Cl atoms. For this reason, the yield decreases with increasing consumption of C_2H_6, and the true yield is obtained by extrapolating the data to zero consumption. The yields of C_2H_4 (0.25%) and C_2H_5Cl (1%) have been corrected for secondary consumption using known rate constants for the reaction of each species with Cl because the yields are small

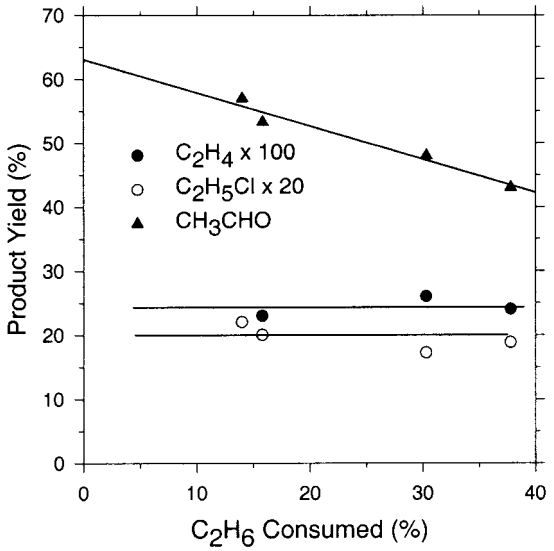

Figure 1. Percentage product yields [(total carbon in product)/(total carbon in the C_2H_6 consumed) × 100] at 298 K as a function of percentage of ethane consumed. Ethanol visible but not quantified (see text). Coated 80 cm^3 reactor.

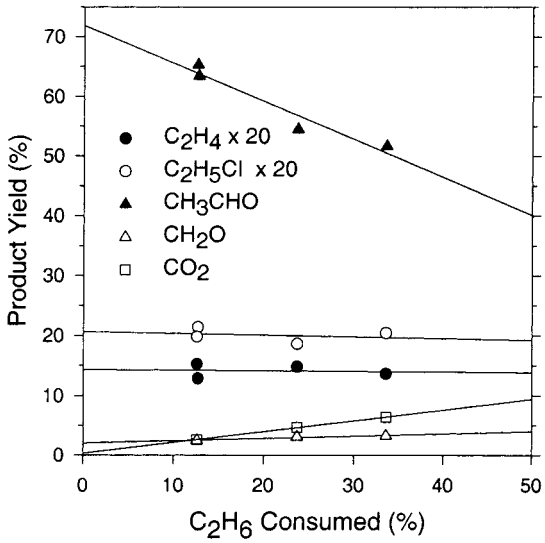

Figure 2. Percentage product yields [(total carbon in product)/(total carbon in the C_2H_6 consumed) × 100] at 425 K as a function of percentage of ethane consumed. Ethanol visible but not quantified (see text). Coated 40 cm^3 reactor; maximum reaction time = 720 s for 33% C_2H_6 consumption.

and the data are noisy at this temperature, rendering extrapolation of little value. The extrapolated yield of CH_3CHO is 63-(±6)% including statistical error (2σ) and estimated calibration errors of the GC. This agrees to within the experimental errors with measured yields of (54 ± 5) and (59 ± 5)% determined by Niki et al.[10] and (54 ± 14)% determined by Wallington et al.[11] Ethanol was present but could not be quantified reliably for reasons stated in the Experimental Section. No GC peak attributable to $C_2H_5O_2H$ was observed although Wallington et al. and Niki et al. determined that the $C_2H_5O_2H$ yield in the reaction is 36 or 30%, respectively. This indicates that $C_2H_5O_2H$ must be lost during either sampling or analysis in the current experiments. One possibility is that it could be transformed into acetaldehyde. However, the sum (CH_3CHO + $C_2H_5O_2H$) represents 85−90% of the total ethane consumed in the experiments by Wallington et al. and by Niki et al., much larger than the CH_3CHO yield (63%) in the current experiments. Thus, the majority of the $C_2H_5O_2H$ must either form another product that is also undetected by the GC analysis, or if it decomposes during the analysis, it may form a very broad GC peak that cannot be seen.

At four elevated temperatures (425, 530, 577, and 640 K), sets of species profiles were also taken as a function of the amount of ethane consumed, allowing extrapolation to zero consumption in order to determine the true yields of the products without the occurrence of secondary reactions. The times of reaction for the maximum consumption of ethane are presented in Figures 2 and 3. This allows a rough estimate of the steady-state chlorine atom concentration at these two temperatures. If it is assumed that the radiation is uniform and that Cl is the only species consuming ethane, $[Cl]_{ss}$ is $\sim 1 \times 10^7$ cm^{-3} at 425 K. This can only be an estimate because the irradiation occurs in a band approximately 0.8 cm wide in a reactor 2.5 cm i.d., and at higher temperatures some ethane consumption could occur via other radicals, particularly OH, which may be present in the irradiated mixture. However, the calculation does provide a rough value for the Cl atom density.

As shown in Figure 2, at 425 K the major product is still CH_3CHO with a yield of 72% of the total carbon present in the ethane consumed. The yield of acetaldehyde again decreases with increasing consumption of ethane because of secondary

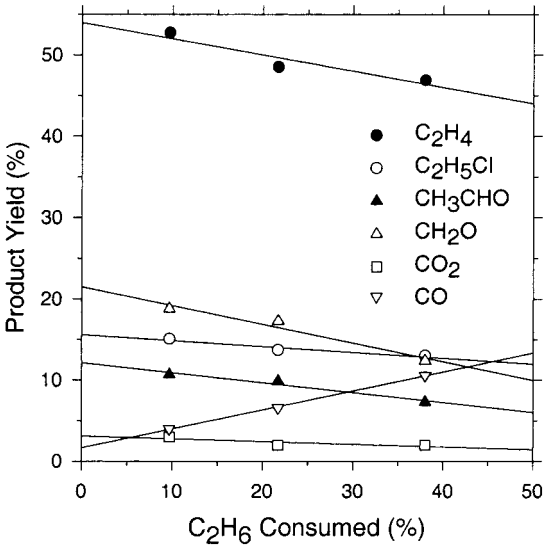

Figure 3. Percentage product yields [(total carbon in product)/(total carbon in the C_2H_6 consumed) × 100] at 577 K as a function of percentage of ethane consumed. No ethanol visible. CH_3Cl yield = 2.4%. Coated 40 cm^3 reactor; maximum reaction time = 420 s for 38% C_2H_6 consumption.

removal by radicals within the reacting mixture, primarily Cl at this temperature as was the case at ambient. CH_2O is the next largest organic species (2.1%), formed by a small amount of thermal decomposition of the ethoxy radical:

$$C_2H_5O + M \rightarrow CH_3 + CH_2O + M \qquad (8)$$

The methyl radical formed in reaction 8 reacts with O_2 producing additional CH_2O (and some methanol) or with Cl_2 forming CH_3Cl (reaction 6). At this temperature, the yields of C_2H_4 and C_2H_5Cl are still small (0.7 ± 0.1)% and (1.0 ± 0.15)%, respectively, although the C_2H_4 has increased significantly. CO_2 is a secondary product resulting from acetaldehyde consumption, as shown by its increasing yield with percentage of C_2H_6 consumed. It has a zero initial yield to within experimental error. CO is visible in the products for 34% ethane consumption but is <1% at 12% consumption. Thus, CO also

has essentially a zero initial yield, and the sum of the measured products represents 76% of the total carbon present in the ethane that has been consumed. Again ethanol was observed but not quantified.

Figure 3 presents the yield curves for the products at 577 K. At this temperature, the acetaldehyde yield (12% of the total carbon in the ethane consumed) has decreased significantly, while those of ethylene (54%), ethyl chloride (15.6%), and formaldehyde (21.5%) have increased sharply. Using the mechanism in Table A-1, the predicted yields at 577 K are: C_2H_4 (53%), C_2H_5Cl (16%), CH_2O (21.5%), CH_3CHO (9.5%), and C_2H_5OH (0.04%). The simulation assumes that, at this temperature, reaction 4 produces only ethoxy radicals either directly or via $C_2H_5O_2H$ decomposition. The increased CH_2O yield results from the rapid increase in the rate of reaction 8 as the temperature rises (see Table A-1). The C_2H_4 and the C_2H_5-Cl yields will be discussed later. CO is formed primarily as a secondary product from the consumption of CH_2O, while CO_2 (3%) may be a minor primary product at this temperature. No C_2H_5OH is visible. The sum of the yields of C_2H_4, C_2H_5Cl, CH_2O, CH_3CHO, and CH_3Cl (2.4%) represents (105 ± 10)% of the ethane that has been consumed. Thus, the carbon balance is excellent, and undoubtedly little $C_2H_5O_2H$ is formed, since this species was responsible for much of the missing carbon at the lower temperatures as discussed above. At 530 K, the measured initial product yields (as a percentage of the total carbon in the ethane consumed) are: CH_3CHO (41%), C_2H_4 (22%), CH_2O (18%), C_2H_5Cl (7%), and CH_3Cl (1%). Both CO_2 (<2%) and CO (<2%) have negligible yields, and the sum of all of the products equals 89% of the carbon in the ethane consumed. At 640 K, the yields are: C_2H_4 (74.5%);, C_2H_5Cl (22%), CH_3CHO (0.5%), CH_3Cl (0.6%) [$\Sigma = 98\%$]. CH_2O, CO, and CO_2 were not determined at 640 K.

Temperature Dependence of C_2H_4 and C_2H_5Cl Yields. As discussed above, the temperature dependence of the C_2H_4 yield is small between 250 and 450 K and then begins to rise sharply.[6] This earlier paper suggested that the sharp rise occurred as reaction 1 became reversible, causing multiple passes through reaction 1a during the mean lifetime of an ethyl radical, each with a finite probability of forming C_2H_4. This would produce an increase in the apparent yield of ethylene. However, as discussed above, it is also possible that another channel for forming C_2H_4 from the stabilized $C_2H_5O_2$ radical opens. This could be the thermally activated, concerted path (reaction 1c) discussed by Rienstra-Kiracofe et al.,[1] or the multistep channel (eqs 1d, 1d′) discussed by Wagner et al.[9] According to the calculations of Rienstra-Kiracofe et al., the barriers for the thermally activated, concerted, and the multistep channels are 29.4 and 35.6 kcal mol^{-1}, respectively, similar to their calculated endothermicity of the decomposition of $C_2H_5O_2$ back to reactants (30.3 kcal mol^{-1}).

Ethylene yields have been measured over the range 298 to 680 K. The yields from the O_2 reaction channel are obtained by subtracting the C_2H_5Cl formed from the amount of C_2H_6 consumed using the following equation after either a correction (<15%) for secondary consumption of the products or extrapolation of the yields to 0% C_2H_6 consumption:

$$Y(C_2H_4) = [C_2H_4]/\{\Delta[C_2H_6] - [C_2H_5Cl]\}$$

The yields presented in Figure 4 (measured at constant total density) were obtained in the three reactors over a period of two years, showing the excellent reproducibility of these measurements. In addition, they are not affected by heterogeneous reactions, which must be different in the three reactors,

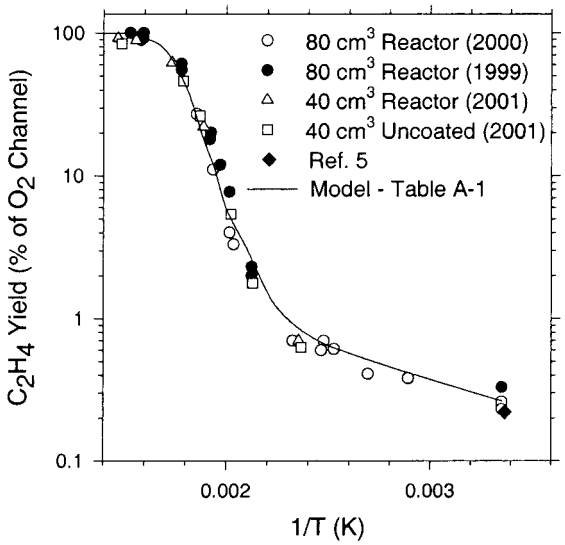

Figure 4. Percentage ethylene yield [(total carbon in product)/(total carbon in the C_2H_6 consumed by reaction with O_2) × 100] from reaction 1 as a function of temperature in each reactor over a period of two years for $M = 6.7 \times 10^{18}$ cm^{-3}.

particularly the uncoated one. The C_2H_4 yield is low at ambient temperature, rises slowly with T until 450 K, and then rises sharply until the yield reaches 100% to within experimental error near 630 K. This behavior is identical to that observed previously,[6] but the present experiments have extended the high-temperature range. The solid line in Figure 4 represents the yield predicted by the mechanism in Table A-1, which is discussed in the Appendix. The 100% ethylene yield is consistent with the 100% HO_2 yield determined at high temperature by Clifford et al.,[7] confirming that at high temperature the overall reaction of O_2 with C_2H_5 yields only these two products to within experimental error. One significant difference in the data from these two experiments is that, in the experiments by Clifford et al., the HO_2 yield curve is shifted ~50 K to higher temperature than in the current experiments. As Clifford et al. have explained, this occurs because their radical densities are higher. A larger radical density will cause the rates of consumption of $C_2H_5O_2$ by bimolecular reactions such as those shown in eqs 2−4 to be faster, and a higher temperature is required before the high-temperature C_2H_4 channel becomes competitive. Testing the current data using the mechanism described in the Appendix indicates that increasing the radical pool concentration from ~ 5×10^{12} molecules cm^{-3} (typical of the present experiments in the range 500−600 K) to 3×10^{13} (typical of Clifford et al.[7]) shifts the predicted C_2H_4 yield profile ~50 K, equal to the shift between the present data and those of Clifford et al. to within experimental error. This calculation was also tested experimentally at 490 K by reducing the UV light intensity a factor of 3.5 (as estimated by a factor of 3.5 reduction in C_2H_6 consumption rate). At the reduced light intensity, the C_2H_4 yield increased by a factor of 1.6. Based on the temperature dependence of the ethylene yield in Figure 4 at this temperature, this is equivalent to a shift in the position of the sharp rise by ~12 K to lower temperature. The model predicts exactly this shift for a factor of 3.5 reduction in C_2H_6 consumption rate.

Figure 5 presents the ratio of the C_2H_4 yield to that of C_2H_5-Cl {$\beta = [C_2H_4]/[C_2H_5Cl]$} as a function of temperature, measured in each of the reactors. All reactors give indistinguishable results, again showing that heterogeneous reactions do not affect the value of β significantly. This ratio provides information about the mechanism of C_2H_4 formation. For temperatures below 450 K, β increases slowly with temperature at constant

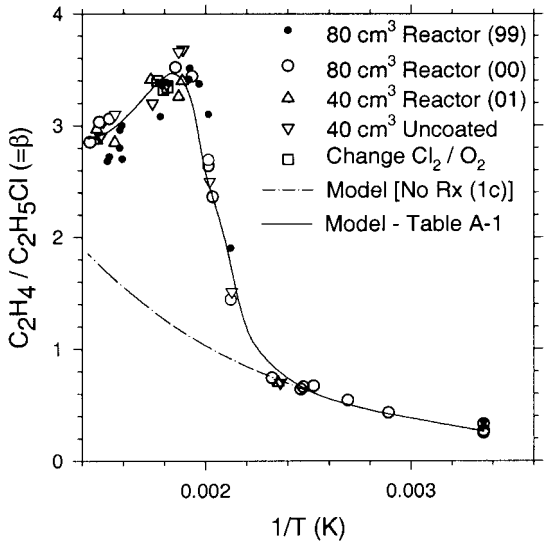

Figure 5. Plot of the ratio ($\beta = C_2H_4/C_2H_5Cl$) as a function of temperature in each reactor over two years ($M = 6.7 \times 10^{18}$ cm^{-3}). Squares show data points at a different Cl_2/O_2 (= 0.013) after correction-to-base ratio (= 0.0044, see text). The solid line presents the β predicted by the mechanism in Table A-1. The dash−dot line shows the β predicted if reaction 1c is removed.

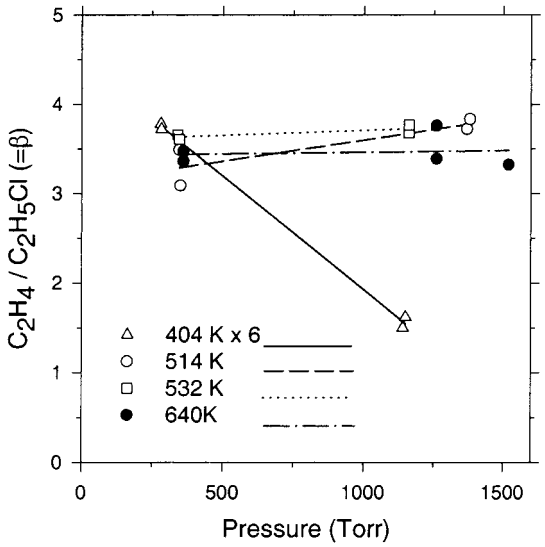

Figure 6. Pressure dependence of the ratio ($\beta = C_2H_4/C_2H_5Cl$) at four temperatures.

density in direct correspondence with the increase in C_2H_4 yield while the C_2H_5Cl yield remains essentially constant (0.9 ± 0.15%). The ethylene yield increases with temperature either because there is a small barrier to reaction 1a or because, as the temperature increases, more energy is deposited into the chemically activated $C_2H_5O_2$* radical.[9] On the basis of the ab initio transition state barrier calculations, in which the transition state of reaction 1a lies below the reactants, the latter explanation is more likely. This additional energy will make deactivation via reaction 1b somewhat less efficient at constant density as the temperature rises, increasing the C_2H_4 yield (and that of β) as observed. If the formation of C_2H_4 continued to occur solely through the chemically activated adduct (reaction 1a) throughout the entire temperature range, the ethylene and ethyl chloride yields would both increase rapidly above 450 K at similar rates. This would occur because of the multiple passes through reaction 1a and also reaction 7 as reaction 1 becomes reversible, as discussed above. Both products would have the ethyl radical as a direct precursor. Therefore, β would continue to increase approximately along an extrapolation of the ratios measured between 298 and 450 K (dashed−dot curve in Figure 5 estimated by the mechanism discussed in the Appendix) because of the additional energy being deposited in the chemically activated ethyl peroxy adduct and the small negative activation energy of reaction 7.

In fact, β increases sharply between 450 and 500 K. Above 500 K, β reaches a peak and then decreases slowly with increasing temperature by a small but significant amount. This suggests that another channel for formation of C_2H_4 has opened above 450 K, and that, while it remains the precursor of C_2H_5Cl, C_2H_5 is no longer the sole precursor of C_2H_4. Support for this statement can be found in the pressure-dependent data in Figure 6. In these pressure-dependent experiments, the densities of C_2H_6, Cl_2, and O_2 remained constant, and N_2 was added to vary the pressure. At 404 K, which is below the break temperature in the β curve, there is a strong dependence on pressure, consistent with reaction 1a as the major source of C_2H_4. The pressure dependence of β from the limited data in Figure 6 at 404 K is approximately $P^{-0.7}$, similar to the $P^{-0.8}$ observed for the C_2H_4 yield in extensive experiments at 298 K.[5] These observations are consistent with reaction 1a as the source of C_2H_4 and reaction 7, which is independent of pressure, as the source of C_2H_5Cl in the low-temperature region. At 514 K, near the peak in β, there is essentially no pressure dependence to within the scatter of the limited data. At both 532 and 640 K, no pressure dependence is observed; the data at these temperatures are less noisy than those at 514 K because the absolute yields of C_2H_4 and C_2H_5Cl have each risen substantially. The lack of an observable pressure dependence above 500 K supports the contention that another channel for C_2H_4 formation, different from reaction 1a, has opened. That channel could be either reaction 1c, the thermally activated, concerted elimination, or reaction 1d, the multistep mechanism. As a check of the validity of β in Figure 5, three experiments were performed at 555 K with the Cl_2 density increased by a factor of approximately 3, changing the Cl_2/O_2 ratio. This will increase the yield of C_2H_5Cl thereby decreasing β by the same factor, as shown in eq A below. These data are plotted as squares in Figure 5 after being increased by the ratio of Cl_2/O_2 in these three test mixtures to that of the base mixture. These corrected values agree with β for the base mixture at that temperature.

Based on the ab initio calculations of Rienstra-Kiracofe et al.,[1] Miller and Klippenstein,[2] and Sheng et al.,[3] both of these channels (eqs 1c and 1d) have barriers similar to the endothermicity of reaction −1, the decomposition of $C_2H_5O_2$ back to reactants. Therefore, in either case, β would increase very sharply as the new channel opened and then show a slower temperature dependence related to the barrier height of reaction −1 relative to that of either reaction 1c or 1d. If reaction 1c (or 1d) is the sole source of C_2H_4 beyond the break, both C_2H_4 and C_2H_5Cl now have $C_2H_5O_2$ as a common precursor, and assuming that reaction 1 is equilibrated [K_1(eq)]:

$$[C_2H_4]/[C_2H_5Cl] = k_{1c}[C_2H_5O_2]/\{k_7[C_2H_5O_2]\,[Cl_2]/K_1(\mathrm{eq})\,[O_2]\}$$

$$= k_{1c}K_1(\mathrm{eq})\,[O_2]/k_7[Cl_2] \qquad \text{(A)}$$

$K_1(\mathrm{eq}) = A\exp(-\Delta H_1/RT)$ and $k_{1c} = B\exp(-E_{1c}/RT)$, where ΔH_1 is the heat of reaction of reaction 1 and E_{1c} is the activation energy of reaction 1c. The rate constant k_7 has a small negative activation energy [$k_7 = 1.26 \times 10^{-11}\exp(302 \pm 230/RT)$].[12] Based on this simplified analytical expression, the temperature

dependence after the break would be $\beta \sim \exp[-(\Delta H_1 + E_{1c})/RT)$. Thus, β would exhibit a negative temperature coefficient for temperatures higher than its peak if $|\Delta H_1| > E_{1c}$, as is predicted in all three theoretical studies.[1-3] However, it is difficult to assess the potential errors in the calculated relative transition state energies for reactions 1c and 1d (estimated to be ±2 kcal at the level of theory used by Rienstra-Kiracofe et al.[13]). This simplified expression ignores other reactions in the system, and the full mechanism will be discussed in the Appendix.

Equation A is a simplified expression which assumes that either reaction 1c or 1d is the only source of C_2H_4 above 500 K. In fact, C_2H_4 will continue to be generated by reaction 1a throughout the entire temperature range, and C_2H_4 yields from all three sources will increase sharply above 450 K. The ratio β will change sharply because additional channels for C_2H_4 formation open while C_2H_5Cl is formed via the same channel throughout the temperature range studied. Therefore, the temperature dependence of β has been fitted by a chemical mechanism presented in Table A-1 and discussed in the Appendix. This mechanism uses experimental rate constants or rate constants estimated from other data for all reactions except reactions 1a, 1c, and $K_{1\,eq}$, which have been fitted to the experimental data. The predicted curve for β is presented as a solid line in Figure 5 and agrees well with the data throughout the entire temperature range. The excellent agreement with the experimental data provides evidence that a reaction channel to form C_2H_4, different from eq 1a, opens above 450 K. Rate constants for reactions 1a, 1c, and for $K_{1\,eq}$ derived from the current experiments are discussed in the Appendix.

The data also provide a method for estimating the variation in the importance of reaction 1c relative to reaction 1a [$\chi = C_2H_4(1c)/C_2H_4(1a)$] as the temperature is varied. On the basis of data in Figure 5, experimental values of χ can be estimated from the equation

$$\chi = (\beta - \beta_{1c})/\beta_{1c}$$

In this equation, β_{1c} {$= [C_2H_4(1c)]/[C_2H_5Cl]$} represents the contribution by reaction 1c to β (dash−dot line in Figure 5), and $\beta \equiv \beta_{1a} + \beta_{1c}$. At 530 K, where the peak in β occurs, $\beta_{1c} = 1.15$ and $\beta = 3.45$. Therefore, $\chi = 2.0$. Other values of χ based on the model calculations are: 400 K (0.01), 450 K (0.3), 500 K (1.5), 530 K (1.9), 550 K (1.8), 600 K (1.2), 650 K (0.8), 700 K (0.6). For temperatures below 400 K, essentially all of the C_2H_4 is formed via the chemically activated channel. Beginning near the break in the β curve as a function of temperature, the contribution of the thermally activated, concerted channel (eq 1c) increases sharply, reaching a maximum near 530 K, where the modeled value of β reaches its peak. Above this temperature, the calculated contribution of reaction 1c begins to decline relative to reaction 1a because reaction 1c has a lower barrier than the reverse reaction (reaction −1) to form $C_2H_5 + O_2$. These are only simulated results based on the reaction mechanism in Table A-1, but they suggest that both reactions are significant sources of C_2H_4 at elevated temperature.

One final observation concerning the lack of pressure dependence in β above 515 K (Figure 6) must be made. In ref 6, a small inverse pressure dependence was observed in the ethylene yield at 530 K. No such pressure dependence in either β or C_2H_4 was observed in the current experiments. The reason for this apparent discrepancy is the fact that in the previous experiments (for simplicity), an unreacted mixture suitable for the highest pressure desired was prepared, and the pressure was varied by changing the amount of this mixture added to the reactor. This changes both the total pressure and the densities of all of the reactants including O_2, which will in turn change the radical concentrations. The difference in oxygen density is the reason that the earlier experiments gave an apparently different result. Addition of N_2 while maintaining the same reactant densities, as done in the current experiments, is the correct way to vary the pressure.

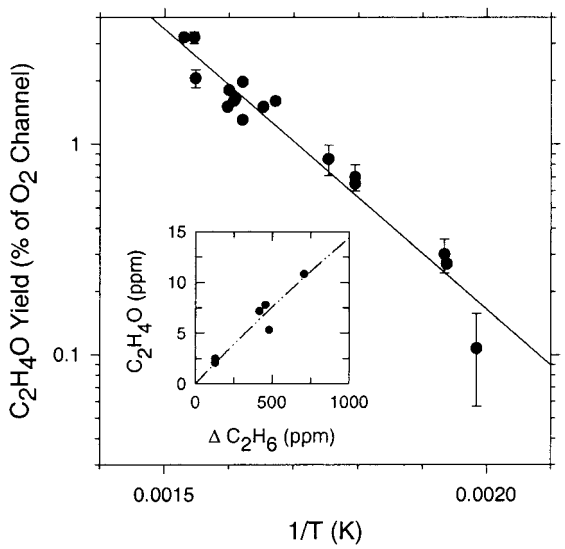

Figure 7. Percentage yield of ethylene oxide (C_2H_4O) from the O_2 channel as a function of temperature. Inset: Mole fraction (ppm) of C_2H_4O formed (*y*-axis) as a function of C_2H_6 consumed (ppm) by O_2 at 624 K.

Yield of Ethylene Oxide. Rienstra-Kiracofe et al.,[1] Miller and Klippenstein,[2] and Sheng et al.[3] have determined that the hydroperoxyethyl radical, which is a stable intermediate in the formation of ethylene by reaction 1d, is also the intermediate species for formation of C_2H_4O from $C_2H_5O_2$,

$$C_2H_4O_2H \rightarrow C_2H_4O + OH \qquad (9)$$

The transition state barriers for the decomposition of $C_2H_4O_2H$ to form C_2H_4 and C_2H_4O in reactions 1d and 9 are similar, suggesting that production of C_2H_4 via reaction 1d should also produce substantial C_2H_4O. To shed more light on the relative contributions of reactions 1c and 1d to the formation of C_2H_4, the yield of ethylene oxide (C_2H_4O) was measured. Initial experiments indicated that C_2H_4O can be lost in a unpassivated reactor, perhaps by heterogeneous processes during the reaction or by problems in sampling. To verify that no loss occurred in the 80 cm^3 passivated reactor, a known small quantity of C_2H_4O was added to the reacting base mixture at several elevated temperatures. No C_2H_4O loss was observed during these tests other than the small amount (<20%) expected from reaction of C_2H_4O with Cl atoms. Figure 7 presents the measured yields of C_2H_4O in the 80 cm^3 reactor as a function of temperature. The yields are small, and the data show a positive temperature coefficient. Because the yield of C_2H_4O at 660 K (the maximum temperature measured) is only ~2.5% of that of the ethylene yield from the O_2 channel of C_2H_5 consumption (as defined in the *Temperature Dependence of C_2H_4 and C_2H_5Cl Yields* subsection), it seems unlikely that reaction 1d is a major source of the C_2H_4. Support for this statement can be found in the theoretically derived rate coefficients for reactions 1d and 9[3] in which the calculated ratio $k_{1d}/k_9 \approx 1.5$ in the 550−700 K range. This suggests that the yields of C_2H_4 and C_2H_4O from these channels should be of similar magnitude. Since the yield of C_2H_4

at 660 K is nearly 100% of the O_2 reaction channel, this indicates that the formation of C_2H_4 from reaction 1d is a minor contributor assuming the calculated relative values of k_9 and k_{1d} are correct to within an order of magnitude. The data in the inset to Figure 7 present the mole fraction (ppm) of C_2H_4O generated for the base mixture as a function of the C_2H_6 consumed by O_2 reaction at 640 K. The plot is linear to within the data scatter, and, therefore, C_2H_4O is likely to be a primary product formed in small yield.

Carbon Balance. The measured yields of the organic species at 577 K in Figure 3 provide another piece of circumstantial evidence concerning the relative importance of reactions 1c and 1d. At this temperature, the sum of all of the measured organic products represents 105(±10)% of the carbon consumed as ethane. CH_3CHO and CH_2O, both formed from the CH_3CH_2O radical, are present at total carbon yields of 12% and 22%, respectively. Based on this observation, approximately 1/3 of the $C_2H_5O_2$ radicals react to produce these oxygenated products. If $C_2H_4O_2H$ were formed via the multistep reaction 1d, addition of O_2 to this alkyl radical forming another peroxy radical, $O_2C_2H_4O_2H$, would be expected to occur,

$$C_2H_4O_2H + O_2 \leftrightarrow O_2C_2H_4O_2H \qquad (10)$$

It is likely that this addition reaction would be exothermic by an amount similar to that of reaction 1, since it involves addition of O_2 to an ethyl radical, albeit with an O_2H group on the carbon atom one removed from the radical site. Based on the equilibrium constant determined for reaction 1 by Knyazev and Slagle,[14] $K_1(\text{eq}) = 1.25 \times 10^6$ bar^{-1} at 577 K. Combining this value with the O_2 partial pressure (0.53 bar) in the present experiments,

$$[C_2H_5O_2]/[C_2H_5] = K_1(\text{eq})\,[O_2] = 6.6 \times 10^5$$

Therefore, at 577 K, ethylperoxy radicals dominate the density of the ethyl radicals assuming that reaction 1 is nearing equilibrium, and it is likely that such would also be the case for the equilibrium of reaction 10. This would provide an opportunity for reaction of $O_2C_2H_4O_2H$ with other peroxy radicals to form oxygenated products not observed from reaction 1, leading to a carbon imbalance at elevated temperature. The fact that the carbon balance is excellent at 577 K, and the products are those expected from reactions of the ethylperoxy radical provides additional support for the absence of reaction 1d as a major channel in the formation of C_2H_4. The carbon balance is also satisfactory at 530 K (89%) and at 640 K (98%). Thus, to within the experimental error, no major products have been missed for temperatures above 530 K.

Net Rate of Reaction 1. The net rate of C_2H_5 consumption by O_2 (reaction 1) relative to its reaction with Cl_2 (reaction 7) can be determined from the yield of C_2H_5Cl relative to the yield of products $[P(O_2)]$ formed via reaction 1: $\{P(O_2) = \Delta[C_2H_6] - [C_2H_5Cl]\}$. These products include oxygenated species and C_2H_4. At low temperature, this represents the rate of the bimolecular reaction 1, since $C_2H_5O_2$ is formed in nearly 100% yield and is a product from which C_2H_5 cannot be reformed,

$$k_1 = k_7[P(O_2)][Cl_2]/[C_2H_5Cl][O_2] \qquad (B)$$

As reaction 1 becomes reversible, however, the net rate of consumption of ethyl radicals to form final products begins to depend significantly on the rate of removal of $C_2H_5O_2$, with which C_2H_5 becomes equilibrated, rather than simply on the direct bimolecular rate constant. Because the formation of C_2H_5-Cl occurs by reaction 7, a direct bimolecular process, the net (apparent) rate constant for consumption of C_2H_5 via reaction 1, k_1(net), can still be deduced from the equation above:

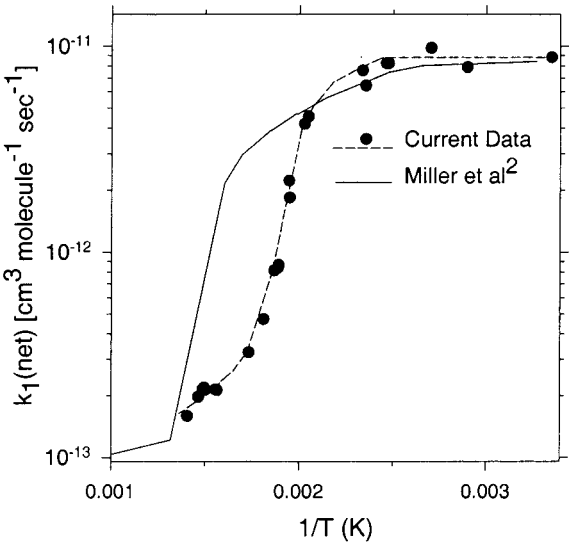

Figure 8. Net rate constant k_1(net) of the reaction $C_2H_5 + O_2$ as a function of temperature (see text). Also shown is the predicted curve from ref 2. The experimental data were obtained using the base mixture defined in the Experiment section.

$$k_1(\text{net}) = k_7[P(O_2)][Cl_2]/[C_2H_5Cl][O_2] \qquad (B')$$

Figure 8 presents k_1(net) as a function of temperature deduced from these measurements (symbols and dashed line). At low temperature, $k_1(\text{net}) = 9.0(\pm 0.1) \times 10^{-11}$ cm^3 molecule^{-1} s^{-1} independent of T, which agrees within experimental error with that measured previously.[8] The net rate then falls sharply starting between 450 and 500 K, where the reverse reaction begins to be significant, reaching a value below 2×10^{-13} at 680 K. Miller et al.[2] predicted a similar phenomenon (see solid line in Figure 8). The reason that their prediction shows the break at higher temperature may be a result of a different definition of the net rate constant from their master equation calculation.

Summary

Cl-initiated rate studies of the reaction $C_2H_5 + O_2$ (eq 1) have been performed relative to $C_2H_5 + Cl_2$ (eq 7) in Pyrex reactors at temperatures between 298 and 680 K at constant density. Under these conditions, the C_2H_4 yield increases slowly with T between 298 and 450 K ($E_a \approx 1$ kcal mol^{-1}). It then rises sharply ($E_a \approx 25$ kcal mol^{-1}) reaching 100% yield from the O_2 channel near 630 K. The ratio C_2H_4/C_2H_5Cl ($= \beta$) shows similar behavior. At temperatures between 298 and 450 K, β increases slowly from 0.3 to 0.8. Between 450 and 500 K, it increases sharply to 3.5 and then falls slowly to 2.8 at 690 K. The temperature dependence of β proves that the mechanism for forming C_2H_4 changes from the purely chemically activated, pressure-dependent reaction 1a for $T < 450$ K to a mechanism including reaction 1a and a new reaction channel at higher temperatures, which is pressure independent. If the reaction continued to proceed via the chemically activated ethylperoxy radical, a sharp increase in the value of β would not occur and pressure dependence would still be present near 500 K. Based on the decrease in β above its peak temperature, this new channel has an activation energy smaller than the endothermicity of reaction −1 (see Appendix) and shows no pressure dependence in the formation of C_2H_4 to within experimental error. If

the multistep path 1d were the principal source of C_2H_4, substantial ethylene oxide would be expected to be present (reaction 9), contrary to the experimental data ($C_2H_4O \sim 2.5\%$ at 660 K), since they share the same precursor radical ($C_2H_4O_2H$). Finally, above ~530 K, the measured carbon balance is 100% to within estimated experimental error, and no new product species are observed that were not present at low temperature. The hydroperoxyethyl radical would be expected to add O_2, forming other products if reaction 1d were a primary source of C_2H_4. Therefore, these data suggest that this new path is the thermally activated, concerted channel studied in detail theoretically by Rienstra-Kiracofe et al.[1] after discovery by earlier members of the Schaefer research group. Both reactions 1a and 1c contribute to the formation of C_2H_4 in reaction 1. The relative rate of formation from these two paths depends on the temperature and pressure at which the reaction takes place. Finally, direct H-atom abstraction is negligible for $T < 700$ K as discussed in the Appendix.

Acknowledgment. Comments by and discussions with A. M. Dean, S. J. Klippenstein, J. A. Miller, J. C. Rienstra-Kiracofe, C. A. Taatjes, W. F. Schneider, and T. J. Wallington have been most welcome and very useful during the preparation of this manuscript. I thank each of them.

Appendix

Model Kinetic Mechanism and Rate Constant Determinations. Table A-1 presents the rate constants used to obtain the fits to the experimental data in Figures 4 and 5. Rate constants that may be pressure dependent at the conditions studied (e.g., k_1, k_{-1}, k_{1a}, k_{1c}) correspond to the total experimental gas density of 6.8×10^{18} molecules cm^{-3}. All rate constants in this mechanism are from literature citations except k_{1a}, k_{1c}, and $K_{1\,eq}$. These three rate constants were adjusted to fit the data in Figure 5. The value of k_{1a} was obtained by fitting the simulated profile of β to the observed experimental data in Figure 5 for temperatures below the break (<450 K), where k_{1c} is negligible because of its high activation energy. The value of k_{1c} was determined by adjusting its preexponential factor and activation energy to obtain the observed peak value and high-temperature fall off in β shown in Figure 5. $K_{1\,eq}$ was adjusted from its literature value to match the location of the sharp rise in β between 450 and 530 K.

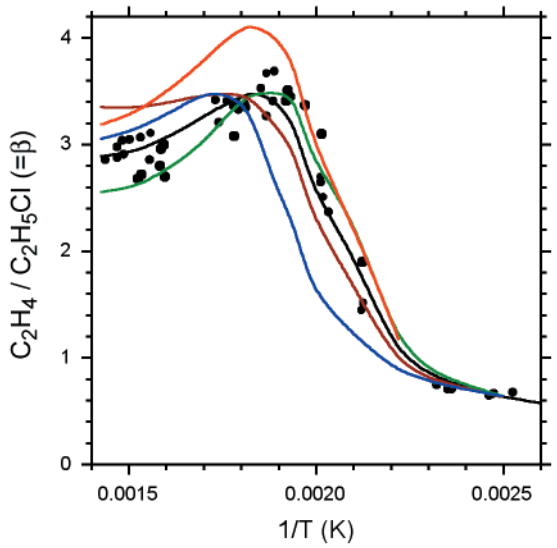

Figure A-1. Effect of the activation energy of k_{1c} and the heat of reaction of reaction 1 on simulated fits to β: individual points, experimental data; black curve, best fit using rate constants in Table A-1; red curve, increase $k_{1c} \times 1.3$; blue curve, K_{eq} from ref 14; brown curve, E_{1c} (activation) = 30 kcal; green curve, E_{1c} = 26 kcal.

Figure A-1 presents all of the measured values of β presented in Figure 5 (dots) as well as the best simulation of the β profile (black line) and simulations obtained by varying k_{1c} and K_{1eq} to show the sensitivity to these parameters. Increasing the A factor of k_{1c} by a factor of 1.3 (red curve) increases the peak simulated value of β by a factor of 1.18 while the shape of the curve remains essentially unchanged, indicating that β is quite sensitive to k_{1c}. The blue curve is obtained by fixing $K_{1\,eq}$ at the value determined by Knyasev and Slagle[14] [$\ln K_{1\,eq}$ (bar^{-1}) = $35470(\pm2000)/RT - 33.58(\pm1.3)/R$]. This curve completely misses the data in the region of rapid rise. To obtain a satisfactory fit in this region, $K_{1\,eq}$ was altered by reducing $|\Delta H^o_{298}|$ to 34 kcal mol^{-1}, a change within the stated experimental error that reduces $K_{1\,eq}$ by a factor of ~4.5 in this temperature range. ΔS was unchanged. This expression for $K_{1\,eq}$, which fits the data well, is used in all simulations. The brown and green curves show the simulated fits with the activation energy of reaction 1c (E_{1c}) increased or decreased by 2 kcal,

TABLE A1: Rate Constants Used in Product Simulation

reaction no.	reaction	rate constant	ref
	$Cl + C_2H_6 = C_2H_5 + HCl$	$8.7 \times 10^{-11} \exp(-225/RT)$	15
7	$C_2H_5 + Cl_2 = C_2H_5Cl + Cl$	$1.08 \times 10^{-11} \exp(302/RT)$	12,16[a]
1a	$C_2H_5 + O_2 = C_2H_4 + HO_2$	$3.4 \times 10^{-13} \exp(-1700/RT)$	b
1	$C_2H_5 + O_2 = C_2H_5O_2$	$k_\infty = 3.36 \times 10^{-14}\, T^{0.98} \exp(64/RT)$ $k_0 = 2.34 \times 10^{-18}\, T^{-4.29} \exp(-220/RT)$ $F_{cent} = 0.897 \exp(-T/601)$	2
−1	$C_2H_5O_2 = C_2H_5 + O_2$	$\ln K_{eq} = 34000/RT - 33.58/R$ (atm^{-1})	14[c]
2	$C_2H_5O_2 + C_2H_5O_2 = C_2H_5O + C_2H_5O + O_2$	calculated from ref 17	
3	$C_2H_5O_2 + C_2H_5O_2 = C_2H_5OH + CH_3CHO + O_2$	calculated from ref 17	
5	$CH_3CH_2O + O_2 = CH_3CHO + HO_2$	$6.3 \times 10^{-14} \exp(-1093/RT)$	18
8	$CH_3CH_2O = CH_3 + CH_2O$	$7.9 \times 10^{13} \exp(-21965/RT)$	19
1c	$C_2H_5O_2 = C_2H_4 + HO_2$	$1.8 \times 10^{11} \exp(-28000/RT)$	b
4	$C_2H_5O_2 + HO_2 =$ Products	calculated from ref 17	
	$CH_3 + O_2 = CH_3O_2$	$1.3 \times 10^{-12}\, (T/298)^{1.24}$	20
11	$CH_3O_2 + CH_3O_2 = CH_3O + CH_3O + O_2$	$9 \times 10^{-14} \exp(390/T)$	17
	$CH_3O_2 + C_2H_5O_2 = CH_3O + C_2H_5O + O_2$	1.4×10^{-13}	d
	$CH_3O + O_2 = CH_2O + HO_2$	$7.2 \times 10^{-14} \exp(-2146/RT)$	21
	$HO_2 + HO_2 = H_2O_2 + O_2$	$7 \times 10^{-10} \exp(-6030/T) + 2.2 \times 10^{-13} \exp(820/T)$	17[e]

[a] Calculated from k_7 at 298 K in ref 16 and the temperature dependence in ref 12. [b] Estimated from current data (see text). [c] Calculated from stated K_{eq} which has been adjusted as described in the Appendix. [d] Average of k_2 and k_{11} with no temperature dependence. [e] Assumed pressure independent.

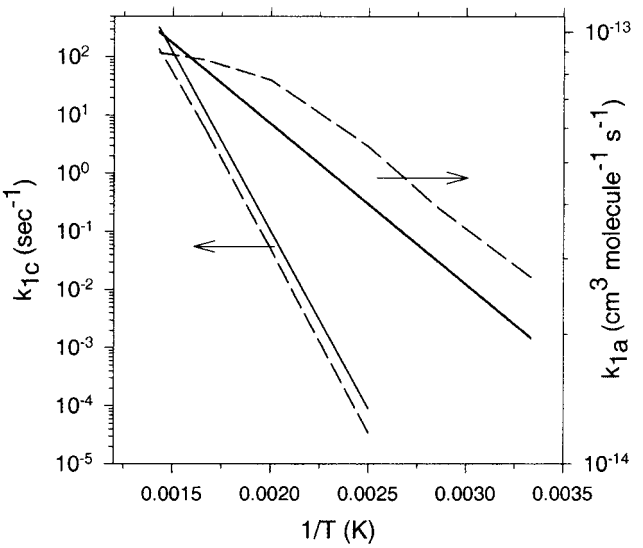

Figure A-2. Comparison of calculated[2] (dashed lines) to experimental (solid lines) values of k_{1c} and k_{1a} as a function of temperature.

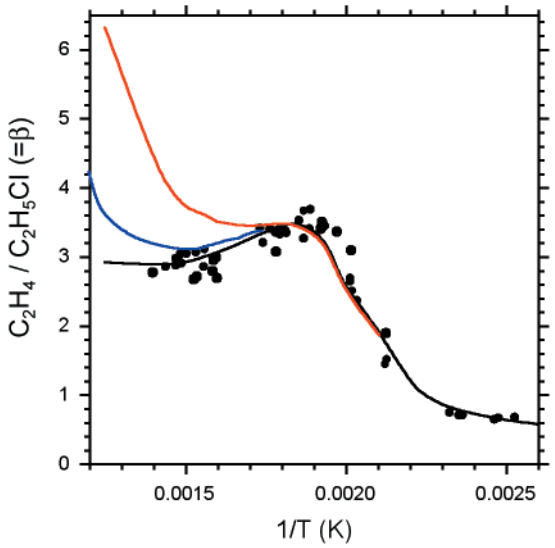

Figure A-3. Model fit using rate constants in Table A-1 with: (1) the addition of the abstraction channel (red curve), $k_{abs} = 1 \times 10^{-10}$ exp(−10000/*RT*) and the A factor of k_{1c} adjusted to 1.66×10^{11} to achieve the observed height of the initial peak in β; (2) the addition of the abstraction channel (blue curve), $k_{abs} = 2 \times 10^{-11}$ exp(−10000/*RT*) and no adjustment to k_{1c}.

respectively. The A factor of k_{1c} was adjusted to yield the experimental maximum value of β in each case. A change of 2 kcal mol^{-1} in activation energy moves the position of the break by a relatively small amount, but it has a very significant effect on the rate of decrease in the value of β at temperatures higher than its peak. The simulation also shows that the rate of decrease depends principally on the difference between the activation energy of reaction −1 and that of the thermally activated, concerted reaction 1c. Based on the combined experimental and simulation results, this difference is 6 ± 2 kcal mol^{-1}, which is somewhat larger than ab initio predicted differences of 1 kcal,[1] 3 kcal,[2] and 5.5 kcal.[3] However, the agreement is reasonable given the difficulty of calculating transition state energies and the correlation between the temperature dependence of reactions 1c and 1a discussed in the next paragraph.

The elementary rate constants for reactions 1a and 1c presented in Table A-1 are compared in Figure A-2 to those deduced from pressure-dependent, theoretical expressions in ref 2 at the density of the current experiments. The predicted value of k_{1c}, the thermally activated path, lies approximately a factor of 2 lower than the value estimated by the fit to the data, while the apparent activation energy is identical to that observed between 400 and 700 K. The predicted (phenomenological) value of k_{1a}, the chemically activated path, agrees with the experimental estimate to within 20% over the temperature range 300−700 K at a density of $M = 6.8 \times 10^{18}$. The predicted rate constant exhibits a near Arrhenius rate expression from 300 to 500 K and then deviates from linearity presumably because of a pressure fall-off in the rate constant as the temperature increases beyond this range. The rate constant in Table A-1 assumes that k_{1a} is purely Arrhenius throughout the temperature range studied. The agreement between the predicted and experimental estimates of these two rate constants is gratifying. If the temperature dependence of k_{1a} does slow above 500 K as predicted by Miller and Klippenstein,[2] then the difference between the activation energies of k_{-1} and k_{1c} would decrease to 4 kcal mol^{-1} to achieve good agreement with the decrease in β for temperatures above its peak value.

H-Atom Abstraction. As discussed by Rienstra-Kiracofe et al.,[1] C_2H_4 formation at high temperature was initially believed to occur via direct H-atom abstraction from the C_2H_5 radical by O_2. Their calculations indicate that this path has an energy barrier >10 kcal mol^{-1} and thus should be of little importance until very high temperature. The mechanism in Table A-1 was used with the addition of a direct abstraction channel to test the importance of this path against data for $T < 700$ K. Two test rate constants were chosen for this reaction: $k_{abs} = 1 \times 10^{-10}$ exp(−10000/*RT*) cm^3 molecule^{-1} s^{-1}, and $k_{abs} = 2 \times 10^{-11}$ exp(−10000/*RT*). The first rate coefficient has a near gas kinetic A factor and an activation energy equal to the lower limit estimated in ref 1. Therefore, it is likely to be an overestimate of the abstraction rate constant. The β curve generated by this mechanism is shown in red in Figure A-3. This curve is essentially identical to the best fit using the mechanism in Table A-1 for temperatures less than or equal to the peak in β (black curve). However, near 600 K, the predicted curve begins to rise as the abstraction reaction becomes a significant source of C_2H_4 and the yield of C_2H_5Cl begins to decrease because of competition from the abstraction reaction. In the 600−700 K range, this model cannot fit the data accurately, indicating that the rate constant of the abstraction reaction must be less than the value chosen. The blue curve is generated by the second (smaller) rate constant for k_{abs}, which represents the largest value that can provide a satisfactory fit to the experimental data. Based on these fits, a conservative upper limit to the abstraction rate constant at 700 K lies near the midpoint of the values used to derive these two curves: k_{abs}(700 K) < 1×10^{-13} cm^3 molecule^{-1} s^{-1}.

References and Notes

(1) Rienstra-Kiracofe, J. C.; Allen, W. D.; Schaefer, H. F., III. *J. Phys. Chem. A* **2000**, *104*, 9823.
(2) Miller, J. A.; Klippenstein, S. J. *Int. J. Chem. Kinet.* **2001**, *33*, 654.
(3) Sheng, C.; Bozzelli, J. W.; Dean, A. M. 2001. Thermochemical Parameters, Reaction Paths and a Detailed Kinetic Model For the C_2H_5 + O_2 Reaction System. Paper No. 100. 2nd Joint Meeting of the U.S. Sections of the Combustion Institute, Oakland, CA; Combustion Institute: Pittsburgh, 2001.
(4) Slagle, I. R.; Feng, Q.; Gutman, D. *J. Phys. Chem.* **1984**, *88*, 3648.
(5) Kaiser, E. W.; Lorkovic, I. M.; Wallington, T. J. *J. Phys. Chem.* **1990**, *94*, 3352.
(6) Kaiser, E. W. *J. Phys. Chem.* **1995**, *99*, 707.
(7) Clifford, E. P.; Farrell, J. T.; DeSain, J. D.; Taatjes, C. A. *J. Phys. Chem. A* **2000**, *104*, 11549.
(8) Kaiser, E. W.; Wallington, T. J.; Andino, J. M. *Chem. Phys. Lett.* **1990**, *168*, 309.

(9) Wagner, A. F.; Slagle, I. R.; Sarzynski, D.; Gutman, D. *J. Phys. Chem.* **1990**, *94*, 1853.
(10) Niki, H.; Maker, P. D.; Savage, C. M.; Breitenbach, L. P. *J. Phys. Chem.* **1982**, *86*, 3825.
(11) Wallington, T. J.; Gierczak, C. A.; Ball, J. C.; Japar, S. M. *Int. J. Chem. Kinet.* **1989**, *21*, 1077.
(12) Timonen, R. S.; Gutman, D. *J. Phys. Chem.* **1986**, *90*, 2987.
(13) Rienstra-Kiracofe, J. C. Private communication.
(14) Knyazev, V. D.; Slagle, I. R. *J. Phys. Chem. A* **1998**, *102*, 1770.
(15) Kaiser, E. W. *Int. J. Chem. Kinet.* **1992**, *24*, 179.
(16) Kaiser, E. W.; Wallington, T. J. *Chem. Phys. Lett.* **1990**, *168*, 309.
(17) Wallington, T. J.; Dagaut, P.; Kurylo, M. J. *Chem. Rev.* **1992**, *92*, 667.
(18) Atkinson, R. *Int. J. Chem. Kinet*. **1997**, *29*, 99.
(19) Hoyermann, K.; Olzmann, M.; Seeba, J.; Viskolca, B. *J. Phys. Chem. A* **1999**, *103*, 5692.
(20) Kaiser, E. W. *J. Phys. Chem.* **1993**, *97*, 11681.
(21) Atkinson, R. *Int. J. Chem. Kinet.* **1997**, *29*, 99.